RESEARCH ON TRANSITIONAL FLOW CHARACTERISTICS OF LABYRINTH-CHANNEL EMITTER

Wanhua Zhao [*] , Jun Zhang, Yiping Tang, Zhengying Wei, Bingheng Lu

[1] *State Key Laboratory for Manufacturing Systems Engineering, Xi'an Jiaotong University, Xi'an, Shaanxi Province, P. R. China 710049*

[*] *Corresponding author, Address: Institute of Advanced Manufacturing Technology, School of Mechanical Engineering, Xi'an Jiaotong University, Xi'an 710049, Shaanxi Province, P. R. China, Tel:+86-29-82665575, Fax:+86-29-82660114, Email: whzhao@mail.xjtu.edu.cn*

Abstract: A physical model for flow characteristics analysis of labyrinth-channel emitter is reconstructed by Reverse Engineering from an injection molded part, and both laminar flow and turbulence models are adopted to simulate the flow state under the condition of low Reynolds numbers. According to the distribution of separation and reattachment points, the onset of transition from laminar to turbulent flow in labyrinth channels occurs at a range of Re=250~300. Furthermore, a visualization system of the flow field inside the labyrinth channels is also established and two kinds of tracers are used in the experiments. The experiment of tracing particles verifies the calculated flow field distribution, and another experiment using dyeing liquor showed the critical Reynolds number characterizing the transition, which is reasonably consistent with numerical simulation results. The critical Reynolds number obtained shows the fact that the flow inside this emitter is turbulent under the pressures of 40~150 kPa.

Keywords: emitter, labyrinth channel, visualization, transitional flow

1. INTRODUCTION

Emitter, one of the key parts in drip irrigation system, is designed to let out the pressurized water in pipes to drop into the soil slowly and uniformly through energy dispassion by its internal structure. The structure has a great

Please use the following format when citing this chapter:

Zhao, W., Zhang, J., Tang, Y., Wei, Z. and Lu, B., 2009, in IFIP International Federation for Information Processing, Volume 294, *Computer and Computing Technologies in Agriculture II, Volume 2*, eds. D. Li, Z. Chunjiang, (Boston: Springer), pp. 881–890.

effect on the hydraulic and anti-clogging performance of emitters, especially for those non-compensating emitters with labyrinth channels. Therefore in recent years, many scholars have carried out the research on the relationship between emitter's structure and performance (macro performance (Wang, et al., 2003; Yao, et al., 2003) and micro performance (Wei, et al., 2006; Zhang, et al., 2007)). In the macro scope, the available experiments such as on flow rate uniformity and relationship between flow rates and pressure heads have been standardized. While, in the micro scope, numerical methods are usually employed due to the intricacy and complexity of emitters. Thus, simulation accuracy mainly depends on the mathematics model. Labyrinth channels, a special structure, differ greatly from the straight channels in terms of their flow characteristics. It is very important for selecting a right mathematical model to explore the transitional flow in the labyrinth channels.

Hence, this paper aims to conduct a numerical study on the transitional flow of an emitter in use, and a flow visualization system is constructed and the flow characteristics can be visualized in labyrinth channels. Experimental results can be used to guide the selection of mathematical model as well as the accuracy verification of numerical simulations.

2. NUMERICAL ANALYSIS ON THE FLOW TRANSITION CHARACTERISTICS

2.1 Physical model and grids system

A kind of labyrinth-channel emitter assembled together with the external pipe system which can be used to carry out the experiments of hydraulic performance is considered. Fig.1 shows the structure stripped from the pipe. In order to measure its dimensions, an optical microscope (VH-8000) and a laser profilometer (Song, et al., 2003) were employed respectively to get the horizontal geometries and the channel depth. The filter grids are considered and the outlet is lengthened a little to obtain a stable flow field, the physical model for numerical analysis is shown in Fig.2.

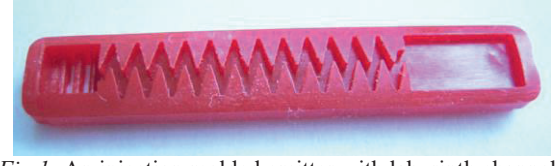

Fig.1: An injection molded emitter with labyrinth channels

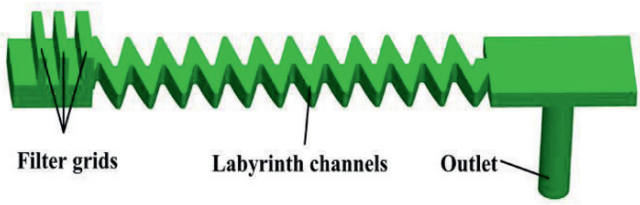

Fig.2: Physical model used for numerical simulations

Considering the sharp turns of the channel boundary, to get high quality grids, physical model was divided into three parts, filter grids, labyrinth channels and outlet. The filter grids and outlet were meshed with structured hexahedron grids, while the labyrinth channels can be meshed with pyramidal grids for their complexity. The regions near the wall and corners were given a finer mesh to simulate the flow field with great velocity gradient. The whole computational domain employed in the computation contained 245,782 control volume cells. From an investigation on the grid independence on the numerical solutions, little influence on the final results was found when using even finer grids.

2.2 Mathematical model

The fluid in the emitter is water, as a result, it is assumed to be viscous, steady, incompressible at room temperature. The fluid gravity and the surface roughness of channel wall are considered while ignoring the surface tension. For the similar structure used in other areas, many scholars have performed a lot of numerical and experimental studies (Nishimura, et al., 1984; Nishimura, et al., 1990) and they all found that the transition from laminar to turbulent flow occurred at a low Reynolds number, e.g. in a range of *Re*=300~500. Therefore in this paper, both laminar flow and turbulence models are applied to explore the flow characteristics under low *Re* values in all cases.

(a) Laminar flow model

The equations of mass conservation and momentum conservation can be expressed as follows:

$$\frac{\partial u_j}{\partial x_j} = 0 \tag{1}$$

$$\rho \frac{\partial}{\partial x_i}\left(u_i u_j\right) = -\frac{\partial p}{\partial x_j} + \frac{\partial}{\partial x_i}\left[\mu\left(\frac{\partial u_i}{\partial x_j} + \frac{\partial u_j}{\partial x_i}\right)\right] \tag{2}$$

Where ρ (kg/m^3) is the fluid density, u_j is the velocity vector in the j^{th} direction.

(b) Turbulence model

There are several turbulence models that can be used, such as standard *k*-*ε*, RNG *k*-*ε*, Realizable *k*-ε, but all of them only calculate the turbulent stress with isotropic turbulent viscosity, and can not take the rotate flow and the variation of surface curvature along the flow direction into account. Here, the flow streamlines are highly turned due to the curved channels, Reynolds Stress Model (RSM) (Mohammad, et al., 2002) is adopted which can accounts for the effects of streamline curvature, swirl, rotation, and rapid changes in strain rate in a more rigorous manner than one-equation and two-equation models. It is a more advanced turbulence model because the turbulent stresses are directly related to the mean velocity gradient. The governing equations involve 12 equations such as Eq. (1), Eq. (2), *k* equation, *ε* equation and the Reynolds stress transport equations (Tao, 2001).

2.3 Boundary conditions and numerical methods

At the inlet of the channel, a uniform fluid velocity may be specified as a boundary condition for the momentum equations according to the flow rate through the emitter under each working condition, this fluid velocity can be obtained from the hydraulic performance experiment of emitters. The outlet condition was treated as standard atmosphere. Turbulence intensity and hydraulic diameter were used to define the turbulence parameters both in inlet and outlet planes. On the wall surface, a value of 0.01 mm was defined as the roughness and the velocity was considered to be zero (non-slip condition), the standard log-law wall function was used in this paper to bridge the near-wall linear sublayer, where acute changes in the fluid velocity are expected. The governing equations were solved by using the SIMPLE algorithm with a segregated solver and a second-order upwind scheme. The CFD program Fluent6.2® was used for the calculations.

2.4 Results and discussion

Fig.3 shows the flow state of different Reynolds numbers in the same channel unit using laminar flow model. Due to the sharp turns (α=31°), a small vortex is developed at the corner of the channel even when *Re*=1 (Fig.3a), while the streamlines are still symmetrical about the central plane of channel unit, which indicates the inertia force is less dominant. As the *Re* increases to 40 shown in Fig.3b, the inertia force also increases and then a phase shift appears between flow streamlines and channel boundary. Moreover, the vortex slowly shifts to the mainstream area and becomes larger. When *Re*=80 as shown in Fig.3c, the first vortex arrives at the middle of the channel, which leaves space for the second vortex. Subsequently, with

the development of the second vortex, flow three dimensionality appears as a result of oscillations of the shear-layer.

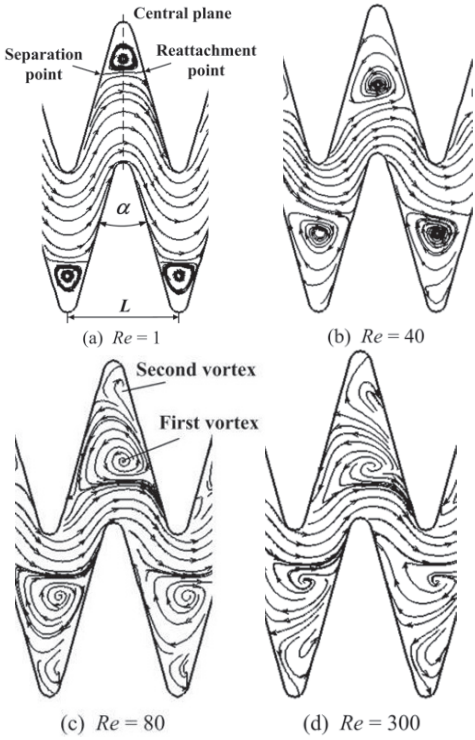

Fig.3: Streamlines in the same channel unit under different Reynolds numbers

Before the fluid reaches the central plane of each unit, the flow separation is developed because of the higher pressure near the outer edge. After the fluid passes through the central plane, the flow reattachment appears due to the opposite pressure gradient plotted in Fig.3a. Fig.4 shows the distribution of flow separation and reattachment points under various Reynolds numbers. In the beginning, the distance between two points become longer as *Re* increases. The flow separation points begin to be stationary when *Re* is more than 40, while the reattachment points tend to be stable at *Re*=100. It can also be concluded from the distribution of the two points that the vortex firstly moves to down left and then to down right corners with the development of *Re*. When *Re* ranges from 250 to 300, the distance between the two points becomes shorter. According to the experimental results performed by Rush (Rush, et al., 1999), the vortex shrinks when the flow transits from laminar to turbulent flow. Thereby, we can also conclude that the transition to turbulence occurs when *Re*=250-300 for this labyrinth

channels. This phenomenon can be partly explained by the theory of pipe flow. The pressure near the outer edge is higher than near the inner edge for the centrifugal force acting on the fluid in labyrinth channels, so it is easier for the vortex and secondary flow to be developed than in straight channel. The intensity and size of the vortices will increase, and they could appear early in this condition, which is helpful for the onset of turbulence.

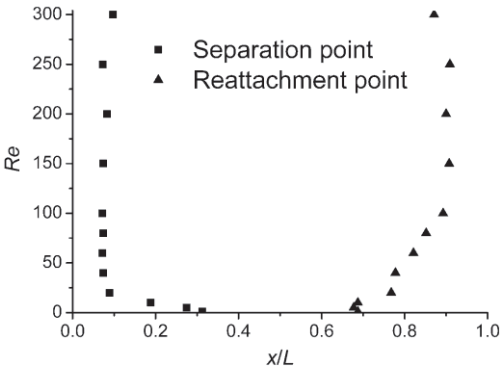

Fig.4: Distribution of separation and reattachment points in the channel unit

3. EXPERIMENTAL TESTS OF THE TRANSITIONAL FLOW CHARACTERISTICS

3.1 Experimental apparatus

The experimental apparatus is shown in Fig.5. A self-priming pump (25WZ-45) is employed as the driven source and a filter with 200 mesh is followed to deal with the large particles in the water. Plexiglass with a thickness of 1 mm is used to make the test model of labyrinth channels because of its excellent transparence. The whole model is consist of three parts, the middle is the contour of the labyrinth channels which is fabricated by CNC carving machine based on 2-D geometry dimensions, and the former and the back are used to fasten and seal the middle part with 8 bolts, as shown in Fig.6. The actual dimensions of the machined model were measured by the optical microscope (VH-8000) and the results show great consistence with the design structure. The high speed video camera (TroubleShooter1000, Fastec Imaging Inc.) was employed to record the flow state. The water passing through labyrinth channels is weighted by an electronic scale, thus the relative *Re* can be calculated.

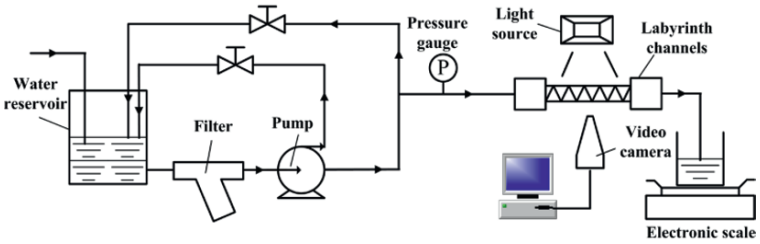

Fig.5: Schematic of the visualization system for the fluid in labyrinth channels

Fig.6: The test model of labyrinth channels fabricated in plexiglass

3.2 Flow visualization methods

Two methods were employed to carry out the experiments. One is the marked particle tracking method, the aluminum powder with a diameter of 5-15 μm was used as the marked particles and its concentration for imaging processing was calculated by the method in the literature (Fan, 2002). In order to prevent the flocculation of particles, a little alcohol was added into the fluid. The other is dyeing liquor method. The ink, used as the dyeing liquor, was filled into an injector with a cubage of 1ml which was fixed at the entrance of labyrinth channels and was parallel with the flow direction.

Considering the influence of dyeing liquor on the observability of labyrinth channels, it is necessary to perform the marked particle tracking experiment firstly and then the dyeing liquor experiment.

3.3 Experimental results and discussion

Fig.7 shows the flow field distribution at *Re*=213, where (a) is from the numerical analysis using laminar flow model, (b) is from the experiment. Except a little noise, the velocity vectors from experiments are consistent with those of numerical analysis. Those noises may be incurred by the error of image processing or the light source which cannot produce the slice light.

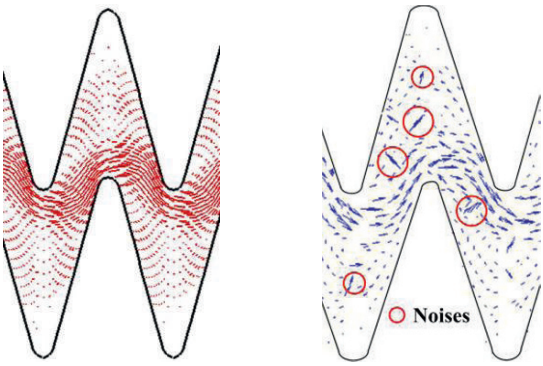

(a) Numerical result (b) Experimental result

Fig.7: The velocity vector when Re=213

The channels in different flow regimes are shown in Fig.8, it indicates the flow states in the same three channel units at different Reynolds numbers. The flow streamlines are still symmetrical about the central plane at low *Re* value such as *Re*=22 (Fig.8a), it can be seen from the width of dyeing liquor that the flow mainly flows along the inside of each unit corner. As Reynolds number increases to 57 (Fig.8b), the flow streamlines shown by the dyeing liquor become narrow, which indicates that the area of mainstream regime is shrunk, in addition, a phase shift appears from here. With the development of *Re* to 93-131, the streamlines begin to diffuse to non-core flow regime as shown in Fig.8c and Fig.8d, the fluid in core and non-core flow regimes intermixed. At *Re*=277 (Fig.8e), the mainstream is getting obscure while at the corner of the channel, the dyeing liquor concentration is increasing. When the flow speed continues to increase (Fig.8f), it becomes difficult to track the flow by dyeing liquor method because of the rapidly decreased definition of dyeing liquor after transition to turbulence which causes a complete mixing with the fluid. Therefore, the present results are consistent with those reported in numerical analysis.

The *Re* is 692 when the emitter is under the pressure of 40 kPa which can be obtained from the experiment of the relationship between pressure heads and flow rates. For this emitter, thereby, the fluid inside the channels has been in the state of turbulence either under the working condition (100 kPa) or in a range of 40-160 kPa that is the experimental scope of relationship between pressure heads and flow rates. As a result, it is more accurate to employ turbulence model to simulate the flow characteristics inside the labyrinth channels.

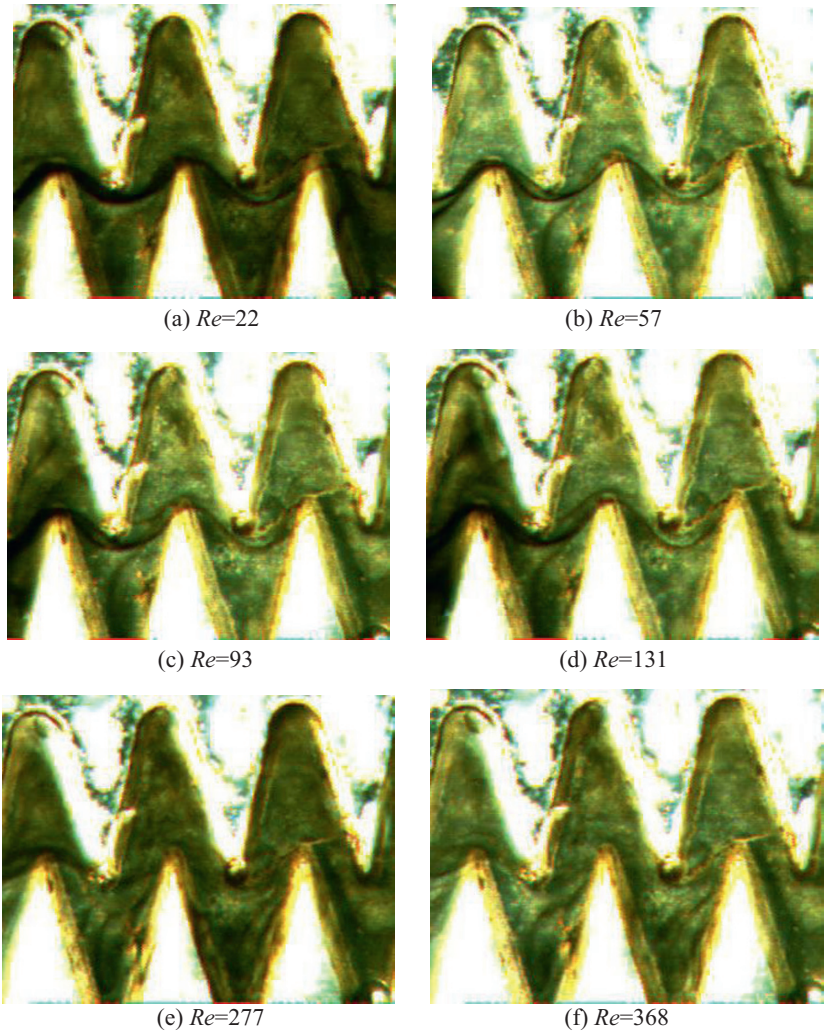

(a) *Re*=22 (b) *Re*=57

(c) *Re*=93 (d) *Re*=131

(e) *Re*=277 (f) *Re*=368

Fig.8: The fluid field visualization by dyeing liquor method

4. CONCLUSION

The transitional flow characteristics in a labyrinth-channel emitter in engineering use were analyzed by numerical simulations and experiments. The results show that various vortexes are developed with the increase of Reynolds numbers for such a labyrinth channel with sharp turns. The transition from laminar to turbulent flow occurs well in advance in the range of *Re*=250-300, which is consistent with the experimental result using dyeing liquor that the critical *Re* is about 277. The result also shows the fact

that the flow inside this emitter is turbulent under the pressures of 40~150 kPa.

ACKNOWLEDGEMENTS

It is gratefully acknowledged that the work presented in this paper is supported by the National High Technology Research and Development Program of China ("863" Program, No. 2002AA2Z4081, 2005AA2Z4040) and the National Natural Science Foundation of China (No. 50275119).

REFERENCES

A. Q. Mohammad, Y J Jang, H C Chen, et al. Flow and heat transfer in rotating two-pass rectangular channels(AR=2) by Reynolds stress turbulence model. International Journal of Heat and Mass Transfer, 2002, 45: 1823-1838

Fan Jichuan. Flow visualization technology in recently years. Beijing: National Defence Industry Press, 2002 (in Chinese)

Song Kang, Zhao Yulong, Jiang Zhuangde, et al. Laser profilometer. Optics and Precision Engineering, 2003, 11(3): 245-248 (in Chinese)

T. A. Rush, T. A. Newell, A. M. Jacobi. An experimental study of flow and heat transfer in sinusoidal wavy passages. International Journal of Heat and Mass Transfer, 1999, 42: 1541-1553

T. Nishimura, S. Murakami, S. Arakawa, et al. Flow observations and mass transfer characteristics in symmetrical wavy-walled channels at moderate Reynolds numbers for steady flow. International Journal of Heat and Mass Transfer, 1990, 33: 835-845

T. Nishimura, Y. Ohori, Y. Kawamura. Flow characteristics in a channel with symmetric wavy wall for steady flow. Journal of Chemical Engineering of JAPAN, 1984, 17: 466-471

Tao Wenquan. Numerical Heat Transfer (2nd edition). Xi'an: Xi'an Jiaotong University Press. 2001(in Chinese)

Wang Ruihuan, Zhao Wanhua, Yang Laixia, et al. Experimental study of the water-saving emitter structure based on rapid prototyping. Journal of Xi'an Jiaotong University, 2003, 37: 542-545 (in Chinese)

Wei Qingsong, Shi Yusheng, Dong Wenchu, et al. Study on hydraulic performance of drip emitters by computational fluid dynamics. Agricultural Water Management, 2006, 84: 130-136

Yao Bin, Liu Zhifeng, Zhang Jianping. Study on the influence of channel length on dripper hydraulic performance. Water Saving Irrigation, 2003, (5): 38-39 (in Chinese)

Zhang Jun, Zhao Wanhua, Lu Bingheng et al. Numerical and experimental study on hydraulic performance of emitters with arc labyrinth channels. Computers and Electronics in Agriculture, 2007, 56:120-129